SUSTAINABLE METHOD TO PREPARE NANOCELLULOSE WITH ENHANCED STABILITY AND STRUCTURAL UNIFORMITY BY USING DEEP EUTECTIC SOLVENTS

FANGJI WU, WOHUA HE, HAOQUN HONG and TAO WEI

School of Materials and Energy, Guangdong University of Technology, Guangzhou 510006, China
✉ *Corresponding author: H. Hong, pshqhong@gmail.com*

Received June 11, 2024

In this study, three different particle sizes of raw materials and four different acidities of deep eutectic solvents (DES) were used to prepare nanocellulose, aiming to find a combination that ensures high yield, good particle size distribution, stability, structural uniformity, and low energy consumption. The effect of DES acidity and feedstock particle size on the prepared nanocellulose was also discussed. The results showed that the greater the acidity of carboxylic acid DES, the smaller the effect of the raw material particle size variation on the yield, and the higher the yield of nanocellulose, the smaller its dimensions, the more uniform its particle size distribution, and the higher its crystallinity. The nanocellulose after this treatment also had carboxylation effects and different esterification due to the acidity differences of the deep eutectic solvent and the structural differences of raw materials. The nanocellulose obtained after these treatments had higher thermal decomposition response.

Keywords: carboxylic acid deep eutectic solvents, ultrasonic crushing, nanocellulose

INTRODUCTION

With the rapid depletion of global energy resources, cellulose, the most abundant renewable natural polymer in nature, has attracted a lot of attention nowadays.[1] The polyhydroxy hydrophilic and multi-branched structure of cellulose[2] determines its physical and chemical properties, leading to its deficiencies in terms of chemical stability, compatibility, strength *etc*.[3] In this case, the nanosizing of cellulose can effectively improve its various properties, such as surface area, compatibility, stability, *etc*.[4]

Different preparation methods are usually chosen for the preparation of nanocellulose according to the desired nanocellulose morphologies. Generally speaking, in the preparation of nanocellulose crystals (CNC), the amorphous zone of nanocellulose is usually hydrolyzed with the help of high hydrogen ion activity of strong acids, leaving nanocellulose with high crystallinity.[4] For achieving cellulose nanofibrils (CNF), the common methods include acid hydrolysis,[5] TEMPO oxidation[6] and others. Generally, a large amount of wastewater is inevitably generated during the utilization of acid hydrolysis, which poses a great challenge to the environmental friendliness of the process. As a green ionic liquid, TEMPO oxidation shows high efficiency in oxidizing cellulose to prepare nanocellulose. However, the waste liquid generated during the oxidation of cellulose is toxic. Besides, there are deficiencies in terms of biodegradability and production cost, which limit its use as a solvent medium.[7]

Deep eutectic solvents (DESs) are formed by two components, a hydrogen donor (HBD) and a hydrogen acceptor (HBA).[8] Usually, we can prepare DES by simply heating these two components.[9] The formed DESs can compete with cellulose chains for hydrogen bonding, causing hydrogen bonding between cellulose chains to break.[10] The DESs are divided into four classes according to the nature of the complexing agent.[11] In carboxylic acid DES, due to the presence of a large number of carboxylic acid molecules and hydrogen ions ionized from the carboxylic acid molecules, this system can form strong hydrogen bonds with choline chloride, which ensures a good treatment result for cellulose.[12] In these different

carboxylic acid DESs, the structural characteristics of the selected HBDs are often different due to the number of carboxylic acids, the degree of hydrogen ionization, and other influences that lead to different characteristics of the carboxylic acid HBDs they constitute.[13] Liu *et al*. found that using a medium-strong acid DES, such as oxalic acid DES, in microwave-assisted DES treatment combined with ultrasonic crushing allowed obtaining a high yield of 74.2% CNCs. Bondancia *et al*. used citric acid treatment to prepare nanocellulose. Due to the low acidity of citric acid, the yield of nanocellulose was not high, but some hydroxyl groups were esterified and carboxylated in the treated nanocellulose.[14]

As noted in previous research reported in the literature, in order to obtain a better processing effect, it is required to subject the raw material to a certain refinement process. Such a process can undeniably improve the treatment of cellulose. However, the relationship between cellulose size and DES acidity in the preparation of nanocellulose has not been explored. Attempting direct nanocellulose preparation from unrefined cellulose can reduce the energy consumption in the nanocellulose preparation process.[15]

In this work, it was aimed to explore the effects of different acidity DESs and different particle sizes of cellulose feedstocks on the prepared nanocellulose related to production yields, microstructures, particle size distributions and stability. We attempted to prepare and analyze nanocellulose from cellulose of different sizes using DES treatment at varying acidity levels in combination with ultrasonic fragmentation. Firstly, MCC, as a fully pretreated product, in powder form, with particle size ranging from 20 um to 80 um, was used as a feedstock. Secondly, bleached coniferous pulp board was selected as a semi-pretreated feedstock, and was subjected to a dispersion treatment, keeping the cellulose lengths in the range of 2 mm-5 mm, considered as long fibers.

Finally, defatted cotton was selected as a non-pretreated raw material, with long cellulose fibers with lengths above 5 mm. Comparisons were made in terms of various aspects, such as yield, XRD, particle size analysis, infrared spectroscopy, and thermal stability analysis.

Finally, further analysis was conducted on the economics of various DESs in production.

EXPERIMENTAL

Materials

Microcrystalline cellulose (MCC) was purchased from Henan Wanbang Industry Co., Ltd. Bleached coniferous pulp board (BCPB) was purchased from Dalian Yangrun Trading Co., Ltd, and defatted cotton (DC) was purchased from Guangzhou Panyu Wanfu Sanitary Products Co. Choline chloride (ChCl) (analytically pure) was purchased from Shanghai McLean Biochemical Technology Co., Ltd., and malonic acid (MA) (analytically pure) was purchased from Tianjin Damao Chemical Reagent Factory. Oxalic acid (OA), citric acid (CA) and urea (Urea) (analytically pure) were purchased from Tianjin Zhiyuan Chemical Reagent Co.

Methods

Pretreatment of raw materials

Microcrystalline cellulose is an industrialized product and requires no pretreatment. A bleached coniferous pulp board needs to be shredded along the cardboard fiber layer. To this end, it was put into a shredder, and deionized water was added to it, operated in the regime 2 minutes on, 3 minutes off, for 10 minutes for effective dispersion of the pulp. Then, the dispersed product was taken out and dried to the appropriate moisture content. Skimmed cotton was simply sheared to ensure that the fiber length remained above 5 mm.

Preparation of DESs

Prior to preparation, choline chloride was dried in an oven at 105 °C overnight. ChCl was mixed with OA, MA and CA in a 1:1 molar ratio in a beaker (the obtained products corresponding to DES-1, DES-2, DES-3, respectively). ChCl and Urea were mixed in a beaker, at a molar ratio of 1:2,[16] and the obtained product was labeled DES-4. Finally, the mixtures were heated and stirred at 80 °C for 1 hour to form the DESs.

Preparation of nanocellulose

The raw materials were put into the DESs in the ratio of 1:50, and heated at 90 °C for 4 h under stirring using a thermostatically heated magnetic stirrer, with the addition of 10 wt% of deionized water, which serves to promote the ionization of the H^+ ions and the departure of Cl^- ions from the domains.[17] Then, the reaction was quenched by using 200 mL of deionized water, and the mixture was vacuum pumped and filtered. After filtration, the filter cake was dispersed in 150 mL-200 mL of deionized water. Then, it was dispersed ultrasonically in an ultrasonicator (Ningbo Juvis Intelligent Technology Co., Ltd., Ningbo, China) at an amplitude of 70% with 2 s on and 1 s off for 1 h. The final suspension was centrifuged at 8,000 r/min several times to obtain the supernatant. The preparation process of nanocellulose is shown in Figure 1.

Testing and characterization

The resulting supernatant was ultrasonically dispersed homogeneously for 10 min. To determine the mass of the CNF suspension, m_{cnf}, a drop of the suspension (m_1) was measured and placed in a Petri dish, then, it was dried for 8 h to form a film with the mass m_2. The mass of the raw material was expressed as m_0. The specific yield was calculated by the formula:

$$yield = \frac{m_{cnf} \times m_2}{m_1 \times m_0} \quad (1)$$

Structural analysis of the diluted and freeze-dried nanocellulose was carried out using an S3400-N scanning electron microscope; scale analysis was performed using a DelsaNano C nanoparticle size and zeta potential analyzer; infrared analysis was carried out using a Nicolet 6700 Fourier Transform Infrared (FTIR) spectrometer, in the scanning range from 4000 to 500 cm^{-1}. Also, an Ultima-IV *in situ* Analytical X-ray diffractometer was used to determine the crystal structure of nanocellulose in the angular range of 2θ = 5-50°,[18] and Segal's empirical method was used to calculate the crystallinity (CrI) of nanocellulose:

$$CrI = \frac{I_{002} - I_{am}}{I_{002}} \times 100\% \quad (2)$$

Thermal stability analysis was carried out using a TGA2, at a heating rate of 10 °C/min in the temperature range of 30-600 °C.

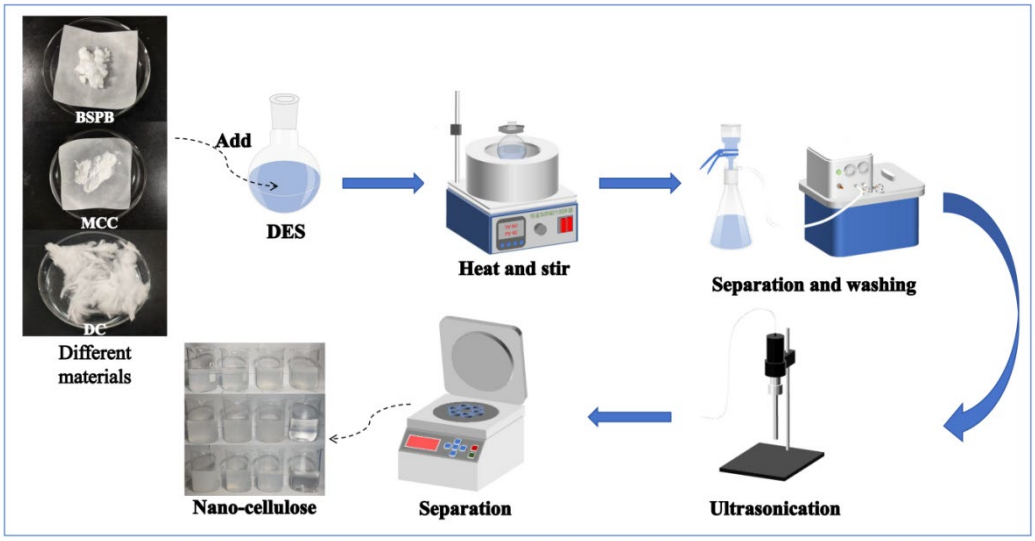

Figure 1: Preparation of nanocellulose by DES treatment, combined with ultrasonication

RESULTS AND DISCUSSION

Acidity of DES aqueous solutions and yield analysis

The prepared DES was diluted to 0.5 mol/L[19] in aqueous solution and then its pH was measured using a pH meter at 20 °C liquid temperature. The specific acidity and the denotation of the DESs are shown in Table 1. It is clear that the acidity of the aqueous solutions of these different DESs corresponds to the magnitude of the acidity of the carboxylic acids that make up the DESs. The aqueous solutions of DESs prepared from medium strength acids, such as oxalic acid, are much more acidic. The acidity of aqueous solutions of DESs composed of two weak acids, *i.e.* malonic acid and citric acid, is also consistent with the acidity of these two weak acids.

Table 2 shows the raw materials used in this study, the DESs, the reaction temperature, the name of the products obtained, with their specific yield. Figure 2 (a) shows the yields of all the samples, while Figure 2 (b) presents the yield obtained after the treatment of the three different feedstocks with oxalic acid DES. It can be seen that, compared with the other three types of DESs, oxalic acid DES still maintains a high yield (52.15%-61.06%) of CNF in the treatment of microcrystalline cellulose, pulp board and cotton due to its high acidity. In contrast to oxalic acid DES, urea-ChCl DES lacks acid assistance in the treatment of virgin fibers due to the absence of carboxylic acids and ionized hydrogen ions from carboxylic acids; the product yields are poor and the particle size of the raw material drastically affects the treatment results. After the treatment of microcrystalline cellulose, the yield of the supernatant left by centrifugation was 15.7%, but in the treatment of non-powdered raw materials, such as pulp board and defatted cotton, the yield was less than 1%.

In Figure 2 (c) and (d), the yields produced by the two carboxylic acid DESs with weak acidity can be seen, after treatment of the three different types of feedstocks. Unlike oxalic acid, which is a medium-strong acid, the two weak acids constituting DESs, because of their low acidity, result in low efficiency of the treatment of the feedstocks. The maximum change in their yields dropped from 28.87% and 26.16% from MCC, to 8.69% and 8.41%, from defatted cotton, for DES-2 and DES-3, respectively.

Table 1
Denotation, aqueous acidity and prices of different DESs used in the study (for 50g)

DESs	DES system	Molar ratio	pH	Prices
DES-1	OA: ChCl	1: 1	0.43	0.68 $/50g
DES-2	MA: ChCl	1: 1	1.15	1.29 $/50g
DES-3	CA: ChCl	1: 1	1.30	0.57 $/50g
DES-4	Urea: ChCl	1: 2	7.35	0.61 $/50g

Table 2
Reaction conditions, CNF denotation and yield for different feedstocks treated with different DESs

No.	Raw material	DES	Temperature (°C)	CNFs	CNF yield (%)
0	MCC	DES-1	90	CNF1	52.15%
1	MCC	DES-2		CNF2	28.87%
2	MCC	DES-3		CNF3	26.16%
3	MCC	DES-4		CNF4	15.70%
4	BCPB	DES-1		CNF5	61.06%
5	BCPB	DES-2		CNF6	25.33%
6	BCPB	DES-3		CNF7	20.02%
7	BCPB	DES-4		CNF8	1%<
8	DC	DES-1		CNF9	55.45%
9	DC	DES-2		CNF10	8.69%
10	DC	DES-3		CNF11	8.41%
11	DC	DES-4		CNF12	1%<

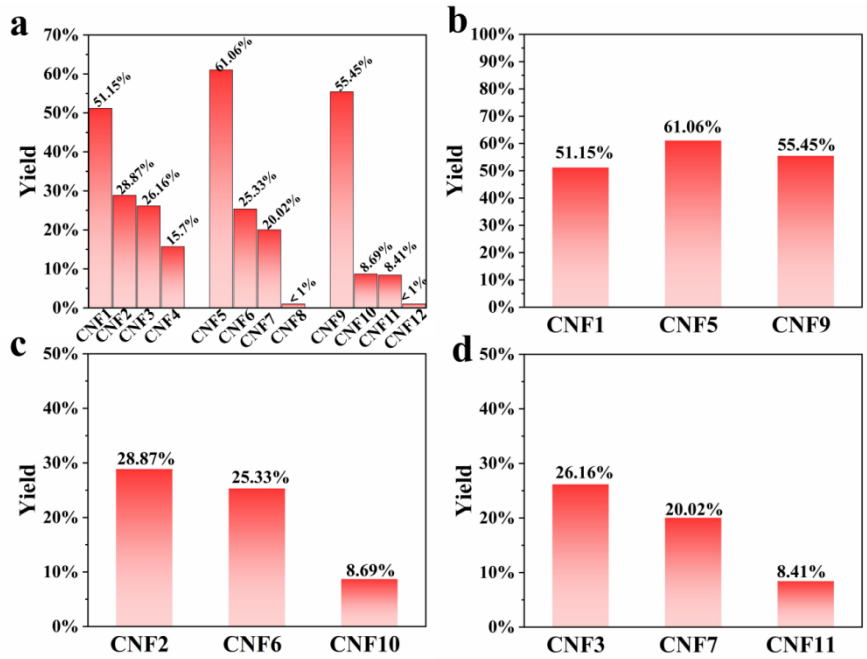

Figure 2: Yields of nanocellulose after different DES treatments (a), yields of nanocellulose after oxalic acid DES treatment (b), malonic acid DES treatment (c) and citric acid DES treatment (d) of three different feedstocks

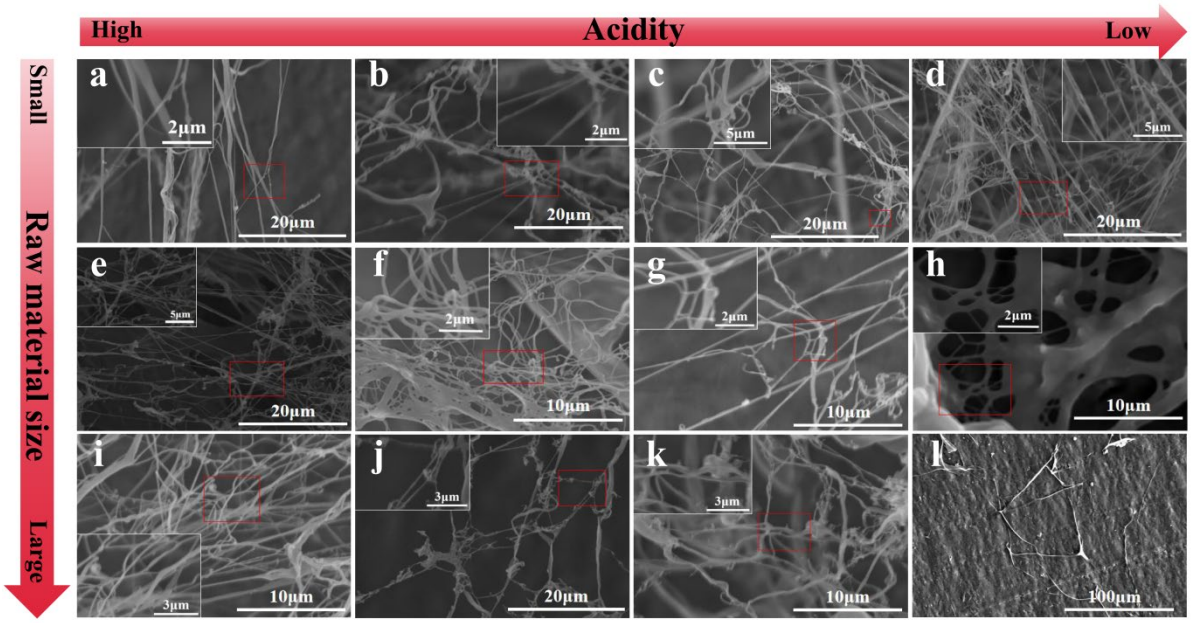

Figure 3: SEM morphology of: MCC treated with ChCl-OA (a), ChCl-MA (b), ChCl-CA (c) and ChCl-Urea (d); BCPB treated with ChCl-OA (e), ChCl-MA (f), ChCl-CA (g), and ChCl-Urea (h); DC treated with ChCl-OA (i), ChCl-MA (j), ChCl-CA (k), and ChCl-Urea (l)

Overall, as the acidity of the DES increases, the concentration of ionized H^+ in the DES also increases. These H^+ ions can effectively facilitate the hydrolysis of cellulose. Thus, the yield of nanocellulose obtained from cellulose treated with DES shows a positive correlation. Interestingly, as the particle size of the cellulose feedstock increases, even though the yield from weak acid DES significantly decreases, the medium-strength acid DES still ensures a good yield, further demonstrating the potential of high-acidity DESs for practical applications.

Microstructural analysis

The microstructures of cellulose from MCC, BCPB, and DC as raw materials after treatments with the four DESs are shown in Figure 3. Most of the treated cellulose presents well-shaped filamentous structure. During the process of freeze-drying the nanocellulose suspensions, they spontaneously orient themselves to form a fiber-sheet structure.[20] Due to the high surface energy of the material and the hydrogen bonding between the nanocellulose, the nanofibrils spontaneously agglomerate and intertwine.[21] Even after dilution and sonication, they retain their cobweb-like screen structure.

Unfortunately, DC, as an unrefined cellulose, exhibits poor homogeneity of CNF and insufficient processing of the CNF after treatment with weak acid DES systems, such as choline chloride-malonic acid and choline chloride-citric acid, due to the insufficient acidity of the DESs. The deep eutectic solvent consisting of choline chloride-urea exhibits an extremely strong influence on the feedstock particle size, compared to the carboxylic acid-based DES. After the treatment of microcrystalline cellulose, the obtained nanocellulose filaments showed good homogeneity. In the use of this class of DES for pulp board and cotton, the cellulose remains relatively intact in its original cellulose form after the treatment, because of the lack of acid-assisted hydrolysis. However, according to Figure 3 (h), the DES formed by choline chloride and urea apparently still acts on the cellulose, thus contributing to the formation of pores on the cellulose surface.

Particle size distribution and stability analysis

The obtained CNF suspensions were subjected to particle size analysis by the Nano Particle Size and Zeta Potential Analyzer. This apparatus can characterize the overall particle size of the samples using the principle of dynamic light scattering. Figure 4 shows the overall intensity-particle size distribution obtained for 12 samples. Almost all of them show normal distribution, except CNF8 and CNF12. As the treatment of cellulose by DESs in CNF8 and CNF12 is not sufficient, the original fiber state is retained. DES treatment still promotes the breaking of hydrogen bonds between cellulose

chains,[22] leading to the formation of holes in the cellulose surface, with fine fibers between the holes. These lead to the formation of a multi-peak distribution that can be demonstrated in the SEM images.

After that, the particle size distribution of each type of CNF below 100 nm was compared according to the pictures. The CNF obtained by oxalic acid-based DES treating BCPB presents finer particle size in this range, which is likely to be related to the presence of multiple treatment processes, such as bleaching, during the preparation of BCPB. However, it is clear that the CNFs obtained by all types of DESs after the treatment of DC, which did not undergo any mechanical refinement, have a poor particle size distribution below 100 nm. Also, they have a gradual increase in the particle size distribution below 100 nm with the decrease of acidity. This is explained by the fact that the size of DC is longer than that of other feedstocks, and more hydrogen ions need to be used to hydrolyze cellulose during DES treatment to form smaller size fibers.[23,24]

The cumulative particle size distribution of different CNFs can be seen in Table 3. It is clear that, although the size of CNFs generated by oxalic acid DES treatment of MCC feedstock is larger, the cumulative particle size distributions of the other two feedstocks at all stages are smaller than those obtained by the rest of the DESs. The polydispersity index (PDI) of celluloses treated by oxalic acid DES is also smaller than those of celluloses treated by other carboxylic acid DESs, and they show good distribution uniformity. These indicate that the unique properties of oxalic acid-based DESs, such as high degree of hydrogen ion ionization, contribute to the efficient preparation of cellulose nanoparticles with uniform size distribution and smaller particle size, compared to those obtained by other carboxylic acid-based and non-carboxylic acid-based DESs. At the same time, as the acidity of DESs increases, the ionization activity of hydrogen ions in the DESs also increases. These hydrogen ions promote the hydrolysis of cellulose, ultimately resulting in a finer cellulose size and a more uniform distribution, which corresponds to the trend in cellulose yield variation. Overall, using high-acidity DESs makes it easier to obtain uniformly sized and smaller nanocellulose fibers. Additionally, this effect does not decline with an increase in the particle size of the raw materials.

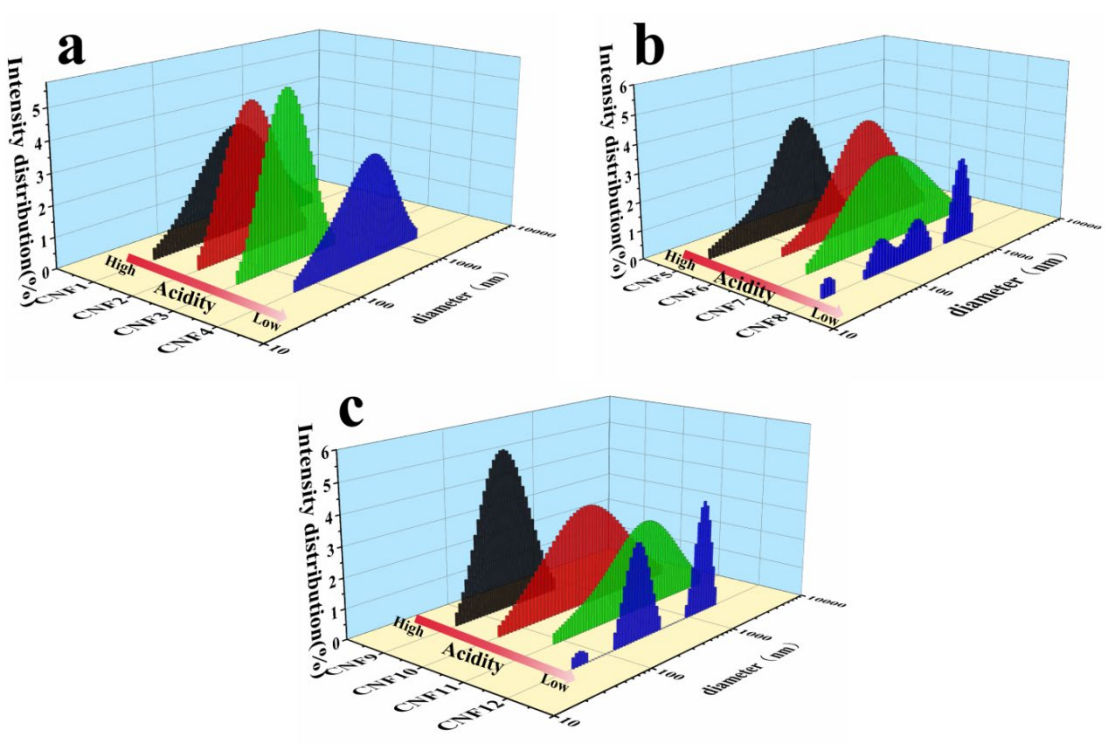

Figure 4: Particle size distribution of CNF suspensions derived from different raw materials: (a) MCC; (b) BCPB; (c) DC

Table 3
Particle size distribution and distribution uniformity of different samples

Sample	D_{10} (nm)	D_{50} (nm)	D_{90} (nm)	PDI
CNF1	90.4	299.0	1014.9	0.252
CNF2	73.6	161.6	368.2	0.281
CNF3	69.0	138.3	280.2	0.285
CNF4	122.1	367.5	901.7	0.198
CNF5	61.0	214.0	755.5	0.162
CNF6	160.6	540.0	1662.8	0.320
CNF7	93.3	356.4	1412.6	0.284
CNF8	127.9	50773.8	70821.1	0.883
CNF9	82.3	166.6	349.6	0.240
CNF10	135.9	519.1	1952.4	0.324
CNF11	202.2	782.5	2424.5	0.344
CNF12	178.3	1534.0	48437.8	0.690

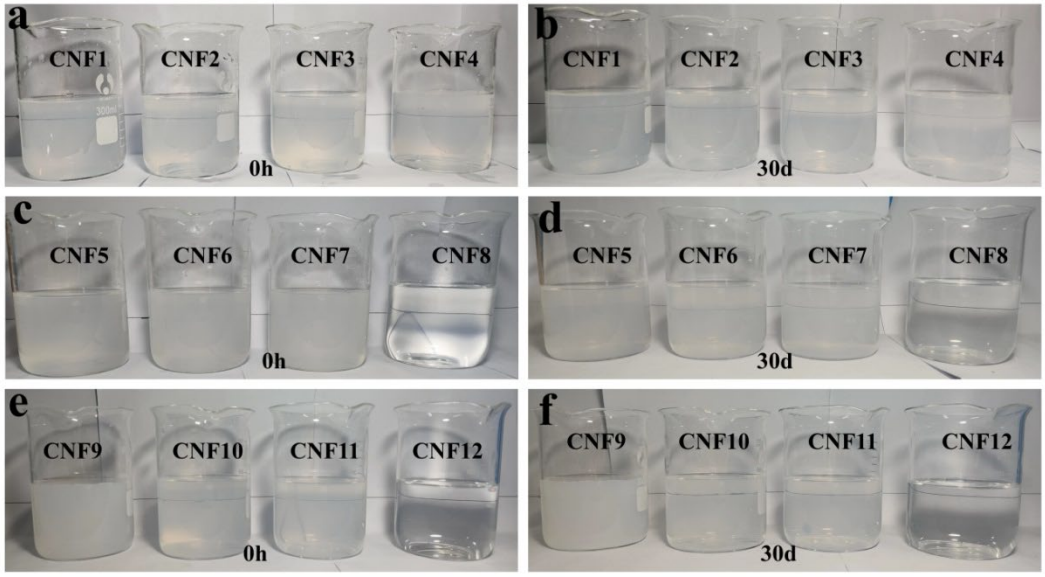

Figure 5: Stability of different CNF suspensions obtained from (a) and (b) MCC after 0 h and 30 days; (c) and (d) BCPB after 0 h and 30 days; (e) and (f) DC after 0 h and 30 days

In Figure 5, the CNF suspensions obtained by ultrasound-assisted refinement and centrifugation after DES treatment are shown. The CNF suspensions were placed on white paper, and most of them showed a mixture of milky white and blue color, with a certain degree of transmittance. Of course, CNF8 and CNF10 maintain a clear water-like transparent color due to the low yield resulting from the urea-based DES treatment of BCPB and DC.

After being left at room temperature for 30 days, neither of the CNF1-CNF12 showed significant sedimentation, the samples maintaining good permeability and demonstrating good dispersion stability. This excellent stability is a further indication that the preparation of the nanocelluloses was successful.

X-ray diffraction analysis

In this analysis, we focused only on the samples with higher yields (all except CNF8 and CNF12), with a sample size of n = 10. The prepared CNFs were characterized by X-ray diffraction to analyze their crystallinity. Crystallinity is the main feature that affects the overall mechanical strength and thermal properties of the polymer. As can be seen in Figure 6, the samples prepared using DESs combined with ultrasonic treatment have characteristic diffraction peaks similar to those of natural cellulose. Two strong peaks were obtained near 2θ=16.4° and 2θ=22.2°, and there was a weak diffraction peak near 2θ=35° for CNF1, CNF2, CNF3, CNF5, and CNF9, which corresponded to cellulose (110), (200)[25] and (004) lattice planes, which are typical cellulose type I structures.[26] They

indicate that the cellulose did not undergo crystalline transition during the process of cellulose treatment with hydrated DESs combined with ultrasonication, and the original cellulose crystalline form was still maintained.

In the MCC material, the crystallinity of the overall carboxylic acid DES did not differ much, and the samples with the largest difference in crystallinity were the CNF obtained from the treatment with oxalic acid DES (61.71% crystallinity) and those obtained from the treatment with malonic acid DES (59.31% crystallinity), with a value of 2.4%. The crystallinity distribution obtained in BCPB and DC showed a positive correlation with acidity distribution. In BCPB materials, the samples with the largest difference in crystallinity were CNF obtained by treatment with oxalic acid-based DES (45.53% crystallinity) and CNF obtained by treatment with citric acid-based DES (39.57% crystallinity), with a difference value of 5.96%. In the DC material, a high crystallinity of 76.91% was obtained by utilizing oxalic acid-based DES as treatment, and the samples with the largest difference in crystallinity were CNF obtained by treatment with oxalic acid-based DES (76.91% crystallinity) versus CNF obtained by treatment with citric acid-based DES (50.2% crystallinity), with a difference value of 26.71%. There is a correlation between the difference in crystallinity and the size of the samples themselves after treatment of the samples with different acidity of carboxylic acid DES.

The ability of different acidity DESs to dissociate H^+ varies. A medium-strength acid – OA – releases more H^+ compared to weak acids – MA and CA, making it easier for acid hydrolysis to occur in the amorphous regions, leading to an increase in crystallinity.[27] Overall, as the acidity of the selected DES increases, the amount of dissociated H^+ in the DES also increases, which facilitates the hydrolysis of the amorphous regions in cellulose and raises its crystallinity.[28] Therefore, selecting a DES with higher acidity for treatment can be useful to prepare cellulose nanofibers with high crystallinity.

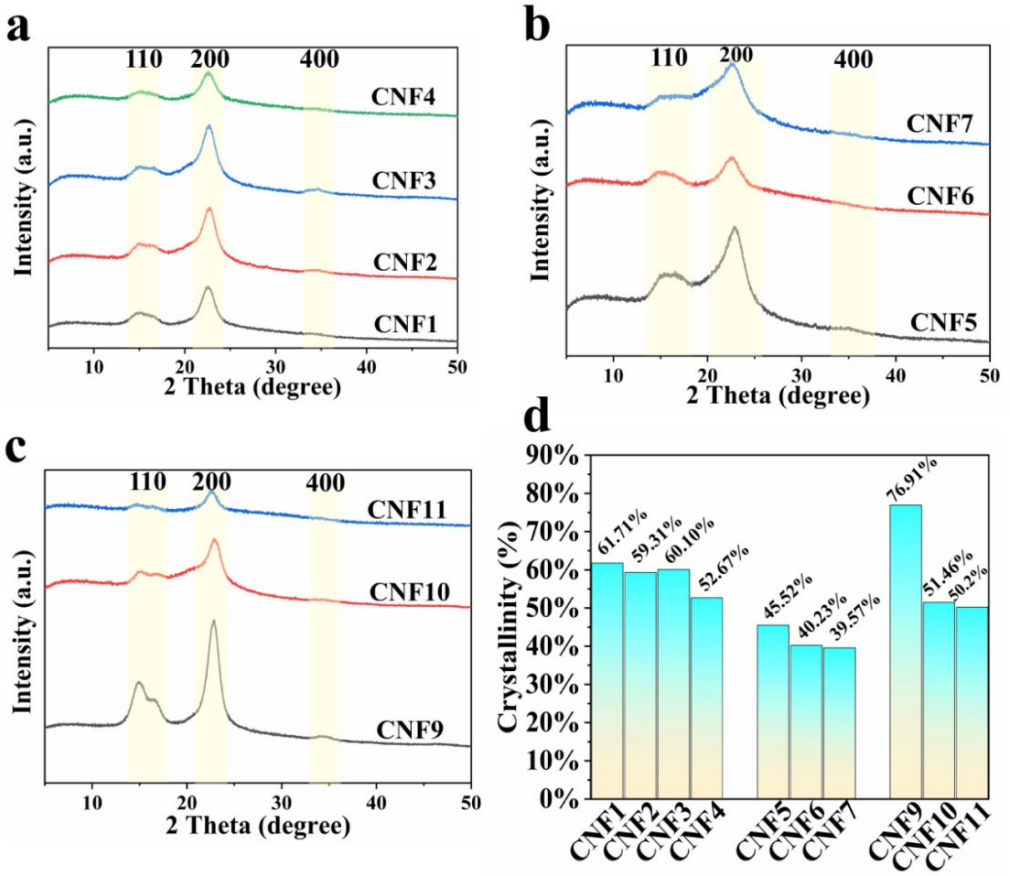

Figure 6: XRD patterns and crystallinity of CNFs obtained from different raw materials: (a) MCC, (b) BCPB, (c) DC; (d) crystallinity of different nanocellulose samples

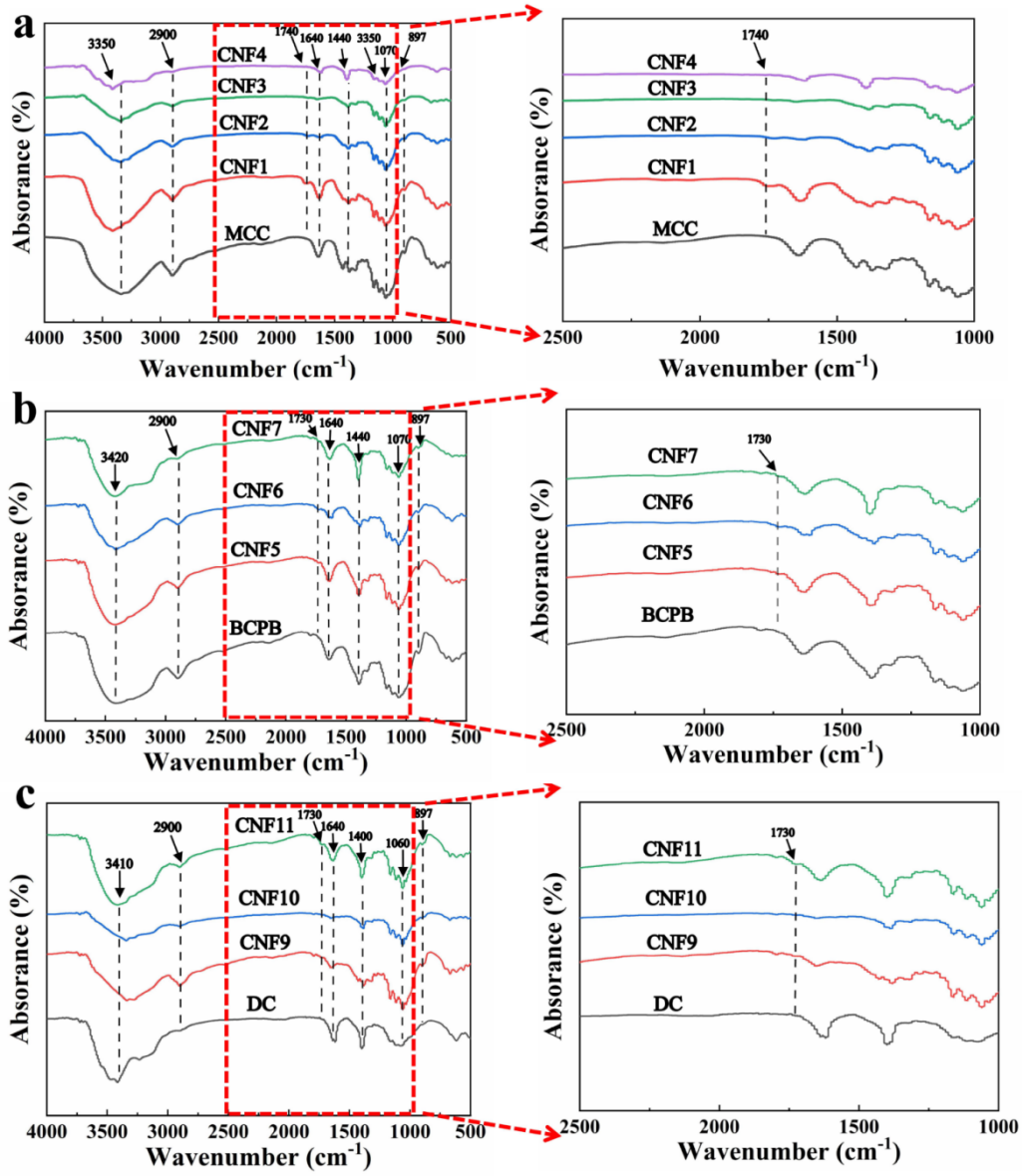

Figure 7: FTIR spectra of CNFs derived from different raw materials: (a) MCC; (b) BCPB; (c) DC

Fourier infrared spectroscopy analysis

In this analysis, samples with higher yields were selected for characterization and the IR spectra obtained are shown in Figure 7. The raw material was also subjected to the infrared spectral analysis as a reference (n = 13). From Figure 7, it is clear that the main characteristic absorption peaks of cellulose are mainly concentrated in the low wavenumber number region (1700-500 cm^{-1}), while in the high wave number region (3650-2800 cm^{-1}), all the samples have two broader peaks (near 3420 cm^{-1}-3350 cm^{-1} versus 2900 cm^{-1}). They are typical cellulose characteristic peaks (O-H stretching vibration in hydroxyl group vs. C-H stretching vibration).[3] In the low wavenumber number region, weak peaks were found near 897 cm^{-1}-899 cm^{-1}, and they are assigned to the C1-O-C4 bond of β-glycosides produced during the dehydration of cellulose.[29] The strong peaks near 1170-1160 cm^{-1} and 1070-1060 cm^{-1} belong to the C-C glycosidic ether bonds of β-1 in the cellulose sample,[30] and C-O-C glycopyranose ring stretching vibration between d-glucose units in cellulose samples, respectively.[31] The peaks at 1640 cm^{-1} for the raw cellulose material and treated CNF represent the O-H bending vibration of air absorbed water.[32]

Unlike the CNF obtained from urea-choline chloride-based DES treatment of feedstock, these carboxylic acid-based DESs lead to an extra weak peak at 1730-1740 cm^{-1}. This peak is an overlap of the carboxylic acid and ester vibrations in

cellulose. During the carboxylic acid-based DES treatment, these acids lead to the carboxylation of a part of cellulose and esterification of a part of cellulose with hydroxyl groups in cellulose, and these carboxylated and esterified groups can produce electrostatic repulsion and assist CNF dispersion.[33]

In these samples, with the change in acidity of DESs and in particle size of the raw material, these IR absorption peaks of esterification and carboxylation changed accordingly. According to Figure 7(a), it is obvious that in the MCC samples, there is a significant peak intensity fluctuation of esterification absorption peaks after treatment with oxalic acid DES. Unfortunately, for malonic acid and citric acid, which are the two weak acids of DESs, the esterification and carboxylation produced by DESs are very weak, and it is even difficult to find the corresponding peak fluctuation in the infrared spectra. The esterification effect of this oxalic acid DES is also significantly weakened along with the increase of the particle size of the material. According to Figure 7(b) and (c), the esterification peaks of CNF5 and CNF9 obtained after oxalic acid DES treatment of BCPB and DC samples are already very weak compared to CNF1. Overall, in combination with IR analysis, the esterification effect of DES declines with decreasing acidity and also with increasing feedstock particle size.

Thermal behaviour analysis

The thermal stability of the 10 higher yield samples was determined using thermogravimetric analysis. The raw material was also included into the thermal performance analysis as a reference (n = 13). In both TG and DTG curves presented in Figure 8, it can be seen that there is a peak at 30-100 °C for all the samples, indicating a large mass loss. This is actually due to the good hydrophilicity, as well as hygroscopicity of the materials, due to the abundance of hydroxyl functional groups of cellulose, which absorb the moisture present in the air. In addition, this is also related to the small molecular compounds attached to the nanocellulose. Evaporation of this moisture and small molecule compounds at the same time as the temperature increases leads to mass loss.[34]

In the temperature range of 200 to 380 °C, the thermal decomposition of cellulose occurs. There are two decomposition peaks on the DTG curve. They are in the ranges of 200-300 °C and 300-380 °C, respectively. The weight loss in the region of 200-300 °C is mainly caused by cellulose glycosidic bond breaking. The decomposition peaks in the temperature region of 300-380 °C are mainly related to structural carbonization and depolymerization of cellulose. After 380 °C, basically the decomposition of cellulose is complete.[20]

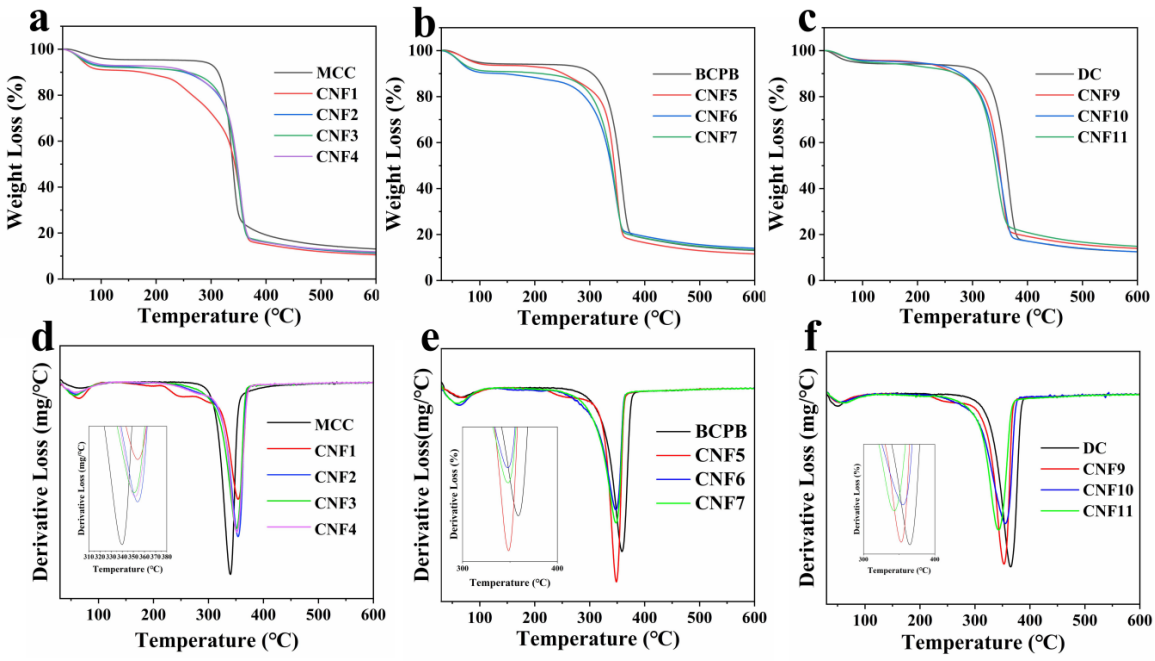

Figure 8: Thermal stability of different CNFs: TG curves of MCC (a), BCPB (b), and DC (c) derived nanocelluloses; DTG curves of MCC (d), BCPB (e) and DC (f) derived nanocelluloses

Table 4
Thermal decomposition onset temperature, maximum thermal decomposition temperature and char residue for different samples

Sample	T_{on} [1] (°C)	T_{max} [2] (°C)	Char yield (%)
MCC	269.5	339.8	13.1
CNF1	142.8	353.9	10.3
CNF2	154.4	354.4	11.1
CNF3	205.1	350	11.4
CNF4	205.6	352	11.7
BCPB	248.3	358.9	13
CNF5	220.1	348.5	11.6
CNF6	231.2	347.8	14
CNF7	237.5	348	13.3
DC	260.4	260.4	12
CNF9	174.4	174.4	14
CNF10	212.5	212.5	12.5
CNF11	228.7	228.7	14.8

T_{on}[1]: Temperature of decomposition onset; T_{max}[2]: Temperature of maximum mass loss rate

In Table 4, the initial decomposition temperature, maximum mass loss temperature, and residual char of the samples are listed. By comparing the initial decomposition temperature, it was found that there was always a faster thermal decomposition response for the samples treated by oxalic acid-based DES. This is caused by several factors, primarily the chemical and physical processes that lead to a reduction in the overall particle size of cellulose. Additionally, higher acidity DESs, such as oxalic acid DES, can dissociate more H^+ ions, resulting in CNF with higher crystallinity and larger specific surface area, which also indicates faster heat transfer. Other factors, such as esterification during the treatment process, will also alter the overall thermal properties of cellulose.[35] Unfortunately, this faster thermal decomposition reaction can have negative effects in certain fields, such as wood-plastic composites and grafting chemistry of cellulose. The inevitable reduction in thermal stability due to factors like increased specific surface area will lead to a decline in the overall thermal performance of the composites. Of course, these issues are not limited to nanocellulose, but pertain to nanomaterials as a whole, and they remain a target for future research.

Economic analysis

Traditional ionic liquids have undergone multiple generations of development. Unfortunately, they remain associated with high costs and significant negative environmental impacts. In contrast, as a new type of ionic liquids, deep eutectic solvents (DESs) offer complete degradability and environmental friendliness, along with a low price, which gives them substantial potential for practical applications. Similarly, when considering how to select deep eutectic solvents for the preparation of nanocellulose, we take into account not only production efficiency, but also the inevitable cost-effectiveness. To be more precise, the cost-effectiveness (ε) is determined as follows:

$$\varepsilon = \frac{c}{q} \tag{3}$$

where c represents the cost incurred during the preparation process ($), and q denotes the total mass of nanocellulose that can ultimately be obtained (g).

In Table 5, we present the costs incurred during the preparation of all nanocellulose types, the final quality obtained, and the resulting cost-effectiveness (note that in this analysis, equipment energy consumption and other factors are kept constant, so they are not considered here). It is clear that due to the lower reagent cost of oxalic acid and higher yield, it offers significantly better cost-effectiveness compared to other carboxylic acid-based DESs for nanocellulose preparation (ranging from $1.1137/g to $1.3039/g), and the particle size of raw materials has little impact on cost-effectiveness.

Table 5
Costs incurred during the preparation of different nanocellulose types, yield obtained, and resulting cost-effectiveness

No.	CNFs	Costs ($)	Yield (g)	Cost-effectiveness ($/g)
1	CNF1	0.68	0.5215	1.3039
2	CNF2	1.29	0.2887	4.4683
3	CNF3	0.57	0.2616	2.1789
4	CNF4	0.61	0.1570	3.8854
5	CNF5	0.68	0.6106	1.1137
6	CNF6	1.29	0.2533	5.0928
7	CNF7	0.57	0.2002	2.8472
8	CNF9	0.68	0.5545	1.2263
9	CNF10	1.29	0.0869	14.8446
10	CNF11	0.57	0.0841	6.7776

CONCLUSION

In this study, the preparation of nanocellulose was carried out using three different raw materials (with various particle sizes) and four different acidities of DESs. The effects of raw material particle size and of the acidity of DESs on the prepared nanocelluloses were compared, and the energy consumption in the preparation of nanocellulose was optimized. The yields of nanocellulose varied considerably after the treatment of the feedstocks with different acidity levels of carboxylic acid DES and non-carboxylic acid DESs. The choline chloride-oxalic acid system showed high yields (>50%) in all three types of feedstocks due to the high hydrogen ion activity; choline chloride-citric acid and choline chloride-malonic acid showed similar yields in feedstocks with different particle sizes due to the similar acidity, but the lower acidity DES treatment would require preliminary refining of the raw material. Choline chloride-urea DES requires a high degree of material refinement. All the feedstocks treated with oxalic acid-based DES showed smaller particle size distribution, more uniform cellulose filament structure, and higher crystallinity, and the nanocellulose obtained showed good dispersion stability, as confirmed by particle size distribution, stability analysis, and XRD characterization. This particle size distribution, along with the higher crystallinity, resulted in a faster thermal decomposition response of the nanocellulose. Meanwhile, the pairing of oxalic acid DES with cotton, a non-refined cellulose, can reduce the need for a refinement process and improve the efficiency of nanocellulose production.

ACKNOWLEDGMENTS: This work was financially supported by the Research Fund for the Doctoral Program of Higher Education of China, under Grant 20134420120009, and Science and Technology Planning Project of Guangdong, under Grant 2014A010105047.

REFERENCES

[1] Y. Wen, Z. Yuan, X. Liu, J. Qu, S. Yang *et al*., *ACS Sustain. Chem. Eng*., **7**, 6131 (2019), https://doi.org/10.1021/acssuschemeng.8b06355
[2] Z. Han, H. Zhu and J.-H. Cheng, *Food Res. Int*., **156**, 111300 (2022), https://doi.org/10.1016/j.foodres.2022.111300
[3] X. Wu, Y. Yuan, S. Hong, J. Xiao, X. Li *et al*., *Ind. Crop. Prod*., **194**, 116259 (2023), https://doi.org/10.1016/j.indcrop.2023.116259
[4] A. Babaei-Ghazvini, B. Vafakish, R. Patel, K. J. Falua, M. J. Dunlop *et al*., *Int. J. Biol. Macromol*., **258**, 128834 (2024), https://doi.org/10.1016/j.ijbiomac.2023.128834
[5] N. I. Abdo, Y. M. Tufik and S. M. Abobakr, *Curr. Res. Green Sustain. Chem*., **6**, 100365 (2023), https://doi.org/10.1016/j.crgsc.2023.100365
[6] Z. Tang, X. Lin, M. Yu, A. K. Mondal and H. Wu, *Int. J. Biol. Macromol*., **259**, 129081 (2024), https://doi.org/10.1016/j.ijbiomac.2023.129081
[7] X. Chang, N. Mujawar Mubarak, S. Ali Mazari, A. Sattar Jatoi, A. Ahmad *et al*., *J. Ind. Eng. Chem*., **104**, 362 (2021), https://doi.org/10.1016/j.jiec.2021.08.033
[8] B. B. Hansen, S. Spittle, B. Chen, D. Poe, Y. Zhang *et al*., *Chem. Rev*., **121**, 1232 (2021), https://doi.org/10.1021/acs.chemrev.0c00385
[9] E. L. Smith, A. P. Abbott and K. S. Ryder, *Chem. Rev*., **114**, 11060 (2014), https://doi.org/10.1021/cr300162p
[10] J. C. Yuan, R. Huang, L. Y. Jiang, G. D. Liu, P. D. Liu *et al*., *Int. J. Biol. Macromol*., **246**, 125687 (2023), https://doi.org/10.1016/j.ijbiomac.2023.125687
[11] Y. L. Chen, X. Zhang, T. T. You and F. Xu, *Cellulose*, **26**, 105 (2019), https://doi.org/10.1007/s10570-018-2130-7
[12] Y. Wang, H. Liu, X. Ji, Q. Wang, Z. Tian *et al*., *Int. J. Biol. Macromol*., **245**, 125227 (2023), https://doi.org/10.1016/j.ijbiomac.2023.125227

[13] D. Tian, Y. Guo, J. Hu, G. Yang, J. Zhang *et al*., *Int. J. Biol. Macromol*., **142**, 288 (2020), https://doi.org/10.1016/j.ijbiomac.2019.09.100.
[14] Y. Liu, B. Guo, Q. Xia, J. Meng, W. Chen *et al*., *ACS Sustain. Chem. Eng*., **5**, 7623 (2017), https://doi.org/10.1021/acssuschemeng.7b00954
[15] T. J. Bondancia, J. De Aguiar, G. Batista, A. J. G. Cruz, J. M. Marconcini *et al*., *Ind. Eng. Chem. Res*., **59**, 11505 (2020), https://doi.org/10.1021/acs.iecr.0c01359
[16] A. Mnasri, R. Khiari, H. Dhaouadi, S Halila and E. Mauret, *Bioresour. Technol*., **368**, 128312 (2023), https://doi.org/10.1016/j.biortech.2022.128312
[17] C. Campano, R. Miranda, N. Merayo, C. Negro and A. Blanco, *Carbohyd. Polym*., **173**, 489 (2017), https://doi.org/10.1016/j.carbpol.2017.05.073
[18] Y. Ma, Q. Xia, Y. Liu, W. Chen, S. Liu *et al*., *ACS Omega*, **4**, 8539 (2019), https://doi.org/10.1021/acsomega.9b00519
[19] M. Jablonsky, A. Haz and V. Majova, *Cellulose*, **26**, 7675 (2019), https://doi.org/10.1007/s10570-019-02629-0
[20] D. Huang, H. Hong, W. Huang, H. Zhang and X. Hong, *Polymers*, **13**, 3119 (2021), https://doi.org/10.3390/polym13183119
[21] L. Jiménez-López, M. E. Eugenio, D. Ibarra, M. Darder, J. A. Martín *et al*., *Polymers*, **12**, 2450 (2020), https://doi.org/10.3390/polym12112450
[22] A. Mnasri, R. Khiari, H. Dhaouadi, S. Halila and E. Mauret, *Chem. Africa*, **6**, 2297 (2023), https://doi.org/10.1007/s42250-022-00511-4
[23] S. Gharehkhani, E. Sadeghinezhad, S. N. Kazi, H. Yarmand, A. Badarudin *et al*., *Carbohyd. Polym*., **115**, 785 (2015), https://doi.org/10.1016/j.carbpol.2014.08.047
[24] O. Nechyporchuk, M. N. Belgacem and J. Bras, *Ind. Crop. Prod*., **93**, 2 (2016), https://doi.org/10.1016/j.indcrop.2016.02.016
[25] W. Wu, H. He, Q. Dong, Y. Wang, F. An *et al*., *Int. J. Biol. Macromol*., **220**, 892 (2022), https://doi.org/10.1016/j.ijbiomac.2022.08.012
[26] Y. Wu, C. Luo, T. Wang, Y. Yang, Y. Sun *et al*., *Int. J. Biol. Macromol*., **255**, 128123 (2024), https://doi.org/10.1016/j.ijbiomac.2023.128123
[27] X. Bi, J. Guo, J. Wen and C. Yu, *Cellulose*, **30**, 9349 (2023), https://doi.org/10.1007/s10570-023-05443-x
[28] A. Mnasri, H. Dhaouadi, R. Khiari, S. Halila and E. Mauret, *Carbohyd. Polym*., **292**, 119606 (2022), https://doi.org/10.1016/j.carbpol.2022.119606
[29] Q. Lu, L. Tang, F. Lin, S. Wang, Y. Chen *et al*., *Cellulose*, **21**, 3497 (2014), https://doi.org/10.1007/s10570-014-0376-2
[30] A. Pandey, A. S. Kalamdhad and Y. C. Sharma, *Sustain. Chem. Pharm*., **37**, 101373 (2024), https://doi.org/10.1016/j.scp.2023.101373
[31] W. Lei, C. Fang, X. Zhou, Q. Yin, S. Pan *et al*., *Carbohyd. Polym*., **181**, 376 (2018), https://doi.org/10.1016/j.carbpol.2017.10.059
[32] A. Célino, O. Gonçalves, F. Jacquemin and S. Fréour, *Carbohyd. Polym*., **101**, 163 (2014), https://doi.org/10.1016/j.carbpol.2013.09.023
[33] S. Liu, Q. Zhang, S. Gou, L. Zhang and Z. Wang, *Carbohyd. Polym*., **251**, 117018 (2021), https://doi.org/10.1016/j.carbpol.2020.117018
[34] Q. Ma, C. Nie, X. Bu, B. Liu, W. Li *et al*., *Int. J. Biol. Macromol*., **242**, 124879 (2023), https://doi.org/10.1016/j.ijbiomac.2023
[35] P. G. Gan, S. T. Sam, M. Abdullah and M. Omar, *J. Appl. Polym. Sci*., **137**, 48544 (2020), https://doi.org/10.1002/app.48544